Tutor/s

Dr. Sergi Astals Garcia
Departament d'Enginyeria Química i Química Analítica

Grau en Enginyeria Química

Treball Final de Grau

Dissolution kinetics model of a by-product rich in magnesium oxide suitable for struvite precipitation

Pau Botines Ramallo

January 2024

UNIVERSITAT DE BARCELONA

Success is getting what you want, happiness is wanting what you get.

W. P. Kinsella

En primer lloc, voldria donar les gràcies a Verónica Aguilar per ajudar-me de manera que ni amb paraules puc descriure. Moltes gràcies per haver-me ajudat a fer aquest treball, t'estaré eternament agraït per tota la paciència que has tingut amb mi. Seguidament, vull donar gràcies al Dr. Sergi Astals pels esforços que ha fet per ajudar-me i fer-me sentir com a casa al laboratori i per les seves aportacions a aquest treball. A continuació, voldria donar les gràcies als companys del laboratori on s'ha dut a terme aquest estudi pels bons moments que hem passat junts al i perquè gràcies a ells, he tingut la suficient motivació per realitzar aquest estudi. Finalment, voldria donar gràcies a tots els meus amics i amigues i a tots els meus familiars per sempre fer-me somriure un dia més.

CONTENTS

SUMMARY

Phosphorus is a limited resource which availability is gradually depleting. Due to the shortage of phosphorus within the European Union (EU) and the EU's dependence on phosphorus imports, phosphorus has been classified by the EU as a critical raw material. Accordingly, the EU is seeking technologies and alternatives to recover phosphorus. One of the most promising possibilities under study is the recovery of phosphorus present in wastewater through the precipitation of struvite. However, the problem of struvite precipitation is the cost associated with the addition of magnesium and an alkaline reagent. The price of magnesium sources (e.g. magnesium chloride, magnesium hydroxide) is relatively high, thereby imposing economic constraints on the process economic feasibility. Moreover, magnesium also classifies as an essencial raw material for the EU. As a result, cheaper magnesium sources are being sought to carry out struvite precipitation. One of the promising new sources is the utilization of a by-product rich in magnesium oxide (named LG-MgO) from the calcination of natural magnesite. It has already been demonstrated that this by-product can precipitate phosphorus as struvite with a high efficiency (60% - 90%). The problem of LG-MgO utilization lies in the limited knowledge of its dissolution behaviour, with a lack of understanding regarding the release of magnesium and hydroxide ions from this by-product. Therefore, this study develops a dissolution kinetic study for the LG-MgO in both neutral and acidic media, with the aim of helping optimize the LG-MgO dosage and usage. Two kinetic models have been proposed, allowing the calculation of the amount of magnesium dissolved under a wide range of operational conditions. This research provides valuable information for the utilization of this industrial by-product for struvite precipitations by reducing the need for raw materials for struvite precipitation and taking a first step into circular economy.

Keywords: Struvite, phosphorus recovery, MgO dissolution, dissolution kinetics, wastewater treatment, resource recovery, circular economy.

RESUM

El fòsfor és un recurs limitat que cada vegada es va esgotant, fent que el preu d'aquest augmenti dia rere dia. A causa de la mancança de fòsfor dins de la Unió Europea (EU) i la dependència que té l'EU de les importacions d'aquest mineral, el fòsfor s'ha catalitzat com una substància crítica. Per aquesta raó, l'EU busca tecnologies i alternatives per recuperar fòsfor. Una de les possibilitats que s'està estudiant és la recuperació del fòsfor que hi ha a les aigües residuals a partir de la precipitació d'estruvita. El problema d'aquest material és que no és viable precipitar-ho a escala industrial a causa del cost associat a l'addició de magnesi i un reactiu alcalí. El preu de fonts de magnesi (e.g. clorur de magnesi, hidròxid de magnesi) son relativament elevats, imposant limitacions econòmiques a la viabilitat econòmica del procés. A més a més, el magnesi també és una substància essencial per l'EU. En conseqüència, s'estan buscant noves fonts de magnesi on el preu sigui més assequible. Una de les noves fonts que té molt de potencial és la utilització d'un subproducte ric en òxid de magnesi (anomenat LG-MgO) provinent de la calcinació de magnesita natural. Aquest ja s'ha demostrat que pot precipitar fòsfor en forma d'estruvita amb un rendiment elevat (entre 60% a 90%). El problema recau en el poc coneixement que es té sobre com és dissolt el LG-MgO i la manca de coneixements relacionats amb l'alliberament d'ions hidròxid i magnesi del subproducte. Per aquesta raó, aquest treball desenvolupa una cinètica de dissolució del LG-MgO en medis neutrals i medis àcids, amb l'objectiu d'ajudar a optimitzar la dosificació i utilització del LG-MgO. S'han proposat dos models, permetent calcular la quantitat de magnesi dissolt sota un rang ampli de condicions operacionals. En conseqüència, aquest estudi dota de valuosa informació per la utilització industrial d'aquest subproducte per precipitar estruvita, reduint la necessitat de matèria primera, fent un primer pas cap a una economia circular.

Paraules clau: Estruvita, recuperació de fòsfor, tractament d'aigües residuals, recuperació de recursos, economia circular.

SUSTAINABLE DEVELOPMENT GOALS

This study develops a dissolution kinetic study for the LG-MgO, an idustrial by-product that can be utilized for municipal and industrial wastewater treatment. Speficically, LG-MgO can be used to recover phosphorus from wastewater by precipitating it in the form of struvite, which is a slow-release fertilizer that can be used in agriculture. Struvite precipitation also allows reducing the amount of nutrients discharged into the environment, thereby reducing eutrophication risk in water bodies. Accordingly, this master final thesis aligns with the following sustainable development goals:

- **Zero hunger (Objective 2):** Sustainable agriculture is being achieved by using struvite as a fertilizer because this fertiliser does not depend on phosphorus importation or local mining.

- **Clean water and sanitation (Objective 6)**: By obtaining fertilizer from the precipitation of phosphorous in wastewateras struvite, the process facilitates nutrient recovery from wastewater.

- **Decent work and economic growth (Objective 8):** By obtaining an economical and cheap fertilizer using a by-product, we are creating new opportunities and markets for and industrial by-product as well as promoting a circular economy.

- **Life below water (Objective 14):** Recovering phosphorus from wastewater reduces the spread of phosphorus in the environment, thereby mitigating eutrophication.

1. INTRODUCTION

1.1. PHOSPHORUS IMPORTANCE

Phosphorus (P) is a non-renewable resource essential for global food production, and it is an essential ingredient in fertilizers [1]. According to Daneshgar et al. [2], approximately 95% of the global phosphorus production is utilized for the manufacture of fertilizer.

The European Union (EU) depends on over 90% of imports for phosphorus from Morocco, the United States, and Kazakhstan [3,4] as EU has very limited phosphate rock deposits [5]. The availability of existing phosphate rock deposits are declining rapidly. Indeed, it has been estimated that phosphate rock reserves will last between 300 to 400 years [6]. Furthermore, the expenses associated with extracting, purifying, stockpiling, and converting them are rising because the quality and accessibility of currently available phosphate rocks are worsening [7]. The European Commission has included phosphate rock in the list of 20 Essential Raw Materials, for which supply security is at risk and economic importance is high [8].

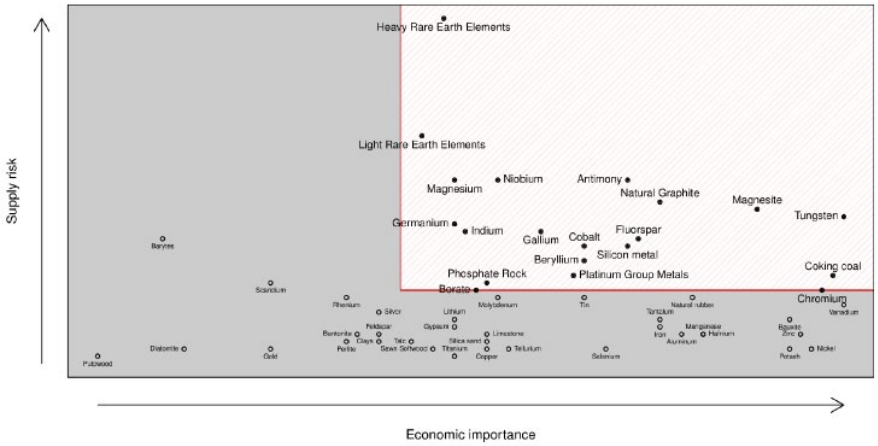

Figure 1. EU list of the 54 critical raw materials. The Raw Essencial Materials are highlighted [5].

Van Dijk et al. [9] showed that one of the largest phosphorus losses within the EU occurs via wastewater, where P recovery from wastewater could represent about 15% of the EU imports. Van Dijk et al. [9] suggested that there is significant potential for phosphorus recovery from municipal sewage. It is estimated that up to 50% of the phosphorus in wastewater could be recovered from the liquid phase while the recovery can reach up to 90% if it is recovered from sewage sludge or sewage sludge ash [10]. This potential recovery, combined with rising expenses and dependency on other countries, encourages the EU to seek technologies that are capable of recovering phosphorus from wastewater.

1.2. PHOSPHORUS TREATMENT IN WATER TREATMENT PLANTS

In the last few years, wastewater treatment plants (WWTPs) have been in charge of controlling the discharge of phosphorus into the environment to prevent water bodies pollution, primarily eutrophication [11,12]. To achieve the discharge concentration limits, WWTPs use several treatments (e.g. phosphorus removal) including physicochemical, biological, algae-based, or a combination of them [13]. WWTPs are where municipal sewage is treated to achieve water quality standards in line with water safety regulations. To achieve the quality standards, the wastewater is subjected to several stages where different treatments take place. The first stage, called the preliminary treatment, prepares the wastewater for the following stages. It mainly consists of removing objects with high dimensions, grease, and sand particles. These are removed because they could damage equipment used in the following stages. The second stage, called the primary treatment, removes suspended solids. During this process, chemicals such as coagulants and flocculants can be added to improve removal of suspended solids. The third stage, also knonw as secondary treatment, is in charge of removing organic matter from the water, as well as nutrients such as nitrogen and phosphorus. This stage generally uses microorganisms to remove these pollutants from wastewater. At this point, the treated water meets the defined discharge requirements and is returned into the environment [14].

The most common process or widely used for phosphorus removal is physicochemical treatment [13], involves adding metal salts (e.g., $FeSO_4$, $AlCl_3$) to the wastewater to precipitate phosphorus with metal ions and forming a highly insoluble precipitates [15]. Although the resultant precipitates may contain a high concentration of phosphorus, the recovery process from this phosphorus can be challenging as the methods studied are very costly [16].

Biological treatments consist of phosphorus-accumulating organisms (PAOs) that remove phosphorus from activated sludge systems [17] and preserve it as polyphosphate in their organism as an energy reserve [18]. Once the phosphorus is removed with PAOs, the sludge formed by these microorganisms can be used because it is a sludge rich in phosphorus. This method is considered an economical and environmentally friendly alternative to physicochemical methods [19].

Algae-based treatments involve using microalgae bioreactors to remove phosphorus from wastewater under specific growing conditions. Similar to PAOs, the retained phosphorus is stored as polyphosphate for energy reserves.

Considering the growing demand for the phosphorus recovery process, one of the most promising methods is the precipitation of magnesium ammonium phosphate hexahydrate ($MgNH_4PO_4 \cdot 6H_2O$), also known as struvite [20].

1.3. STRUVITE PRECIPITATION

Struvite is a slow-release fertilizer with high phosphorus and ammonium content. This mineral can reduce phosphorus concentrations into the environment due to controlled release compared to liquid fertilizers [21]. Phosphorus and nitrogen are nutrients that contribute to plant growth and development. Phosphorus precipitation as struvite precipitation requires that the concentration of magnesium, phosphate, and ammonium in the wastewater exceeds the struvite solubility product constant (K_{sp}) according to Equation 1 [22]. The reported range of pK_{sp} is 12.67 to 14.28 [52,53] where the pK_{sp} is the negative logarithm of the K_{sp}. K_{sp} value depends on several factors, including temperature, pH, ions among others, for this reason, there are different values in the literature [23,24].

$$Mg^{2+} + NH_4^+ + H_nPO_4^{3-n} + 6\ H_2O \rightleftarrows MgNH_4PO_4 \cdot 6\ H_2O + nH^+ \text{ where n = 0, 1 or 2.} \quad \text{(Eq. 1)}$$

The struvite precipitation in WWTPs requires the addition of magnesium because its concentration found in the wastewater is insufficient to exceed the solubility product constant [25]. Martí et al. [26] and Uysal et al. [27] showed that struvite can be efficiently precipitated in a stirred crystallization reactor fed with anaerobic digestion supernatant due to its realtively high phosphate and ammonium concentration. Uysal et al. [27], who used magnesium chloride ($MgCl_2 \cdot 6H_2O$) to

facilitate struvite precipitation, reported that the concentrations of heavy metals and micropollutants present in struvite did not surpass the regulatory thresholds established by the EU in the precipitated struvite.

The main magnesium sources used to induce struvite precipitation are magnesium chloride ($MgCl_2 \cdot 6H_2O$), magnesium oxide (MgO), and magnesium hydroxide ($Mg(OH)_2$) [28]. These salts are dosed to achieve a P:Mg molar ratio between 1:1 and 1:2 [21,22,29,30]. Despite the potential loss of magnesium when using a higher P:Mg molar ratio of 1:1, promoting system oversaturation that enhance phosphorus recovery. Furthermore, the salts are dosed into systems where the pH is adjusted to achieve an optimal pH range using an alkali reagent, typically sodium hydroxide (NaOH) [31]. The optimum pH range for struvite precipitation is between 8 and 9 [29,32,33]. Although different magnesium sources proved to be effective in struvite precipitation, the process lacks economic viability for full-scale implementation [21,22,29,30]. This economic impediment is attributed to the high cost of magnesium salts, which account for approximately 75% of the expenses, alongside other reagents [28]. Additionally, magnesium is included in the EU's crucial primary substances [34]. For these reasons, side/waste stream-derived magnesium sources may present a more cost-effective and desirable alternative for struvite precipitation within the circular economy framework.

1.4. MAGNESIUM RICH BY-PRODUCTS

Different magnesium-rich by-products, such as brine, wood ash, bittern, and low-grade MgO (LG-MgO) have shown potential for making the full-scale struvite precipitation cost-effective [35]. Among these by-products, LG-MgO has been proven effective for struvite precipitation in WWTPs anaerobic digestion supernatants with phophorous recoveries values by means of struvite precipitation ranging between 60% and 90% [35,36,37,38]. LG-MgO is obtained from the calcination of magnesite, which is recovered from air pollution control systems. These systems utilize cyclones to filter the combustion gases from the kiln, resulting in the recovery of fine particles of LG-MgO as by-product. LG-MgO has a heterogeneous composition, including magnesium oxides (MgO), magnesite ($MgCO_3$), calcite (CaCO3), dolomite ($CaMg(CO_3)_2$) amonjg others [39]. The composition of LG-MgO by-product and chemical and physical properties depends on the composition of the raw material and the thermal processes employed in its production [39]. Additionally, LG-MgO is 10 times cheaper than $MgCl_2$ which makes this by-product potentially more cost-effective [35].

Although LG-MgO proved to be effective in the process of struvite precipitation there is limited understanding regarding its dissolution behavior and magnesium liberation. This lack of investigation indicates that the utilization of LG-MgO is not optimizited which could led to significant losses of magnesium in the process. One way to optimize LG-MgO dosage is to understand the dissolution properties of LG-MgO and consequenly the efficacy of struvite precipitation when using LG-MgO.

2. KINETIC STUDY

To develop the kinetic dissolution model, the introduction of theoretical kinetics is undertaken to better comprehend the foundation of this study.

Chemical kinetics is a branch of chemistry that encompasses the investigation of reaction rates which the reactants (R) are transformed into products (P) to understand the kinetic mechanisms for any given chemical reaction [40]. The term "mechanism" is defined as the sequential arrangement of elementary steps that collectively form an overall chemical change. An elementary step denotes the advancement of a reactant or reaction through a singular transition state to a chemical form characterized by a precisely defined and detectable lifetime (Eq. 1) [56].

In instances where the chemical transformation involves multiple elementary steps, the chemical structures that arise after each prociding elementary step, leading up to the eventual formation of the final product, are formally recognized as reaction intermediates (I) (Eq. 2) [41].

$$R \rightarrow P \quad \text{(Eq. 1)}$$

$$R \rightarrow I \rightarrow P \quad \text{(Eq. 2)}$$

The reaction rate is inherently influenced by various factors, including reactant concentration, temperature, contact surface area, and other variables. Kinetic studies are primarily derived on experimental data, wherein initial operating conditions are established, keeping specific variables of interest constant while tracking their effects over time. With the experimental data, kinetic equations that describe the reaction rate can be determined. In addition to experimental measurements, theoretical or computational methods can be used to obtain information about

reaction mechanisms and kinetic parameters, such as rate constants and reaction orders. Two branches emerge depending on the complexity of the reaction: simple kinetics and complex kinetics.

2.1. SIMPLE REACTIONS

The kinetics of simple reactions refers to the study of the reaction rate and mechanism of simple chemical reactions (Eq. 3). In this context, a simple reaction occurs in a single elementary step, meaning it does not involve intermediate stages.

The rate of a reaction is defined as the rate at which reactants are converted into products. It can be expressed in different ways, but it is generally measured as the change in concentration of reactants or products over time. The rate is expressed using a rate equation, which relates the rate to the concentrations of the reactants:

$$\nu_A A + \nu_B B \rightarrow \nu_C C + \nu_D D \quad \text{(Eq. 3)}$$

$$r = k [A]^{\alpha} [B]^{\beta} \quad \text{(Eq. 4)}$$

where:

- ν_A, ν_B, ν_C, and ν_D are the stoichiometric coefficient.
- A and B are the reactants.
- C and D are the products.
- r is the reaction rate (mol/(L·min)).
- k is the reaction rate constant (units depend on the fractional parameters).
- [A], [B], are the concentrations of reactants (mol/L).
- α and β are the fractional parameters.

2.1.1 Temperature dependent term of a rate equation

For many reactions, especially elementary reactions, the rate expression is written as a product of a temperature-dependent term and a composition dependent term. The temperature-dependent term is represented by the reaction rate constant (k). In most cases, the reaction rate constant has been well represented by Arrhenius' equation [42].

The Arrhenius equation introduces the relationships between the reaction rate and a pre-exponential factor (A), activation energy (Ea) and the temperature (T). In simple, single-steps reactions, Arrhenius equation is descibred as it is seen in Equation 5.

$$k = A \cdot \exp(-E_a/RT) \quad \text{(Eq. 5)}$$

where:

- A is the pre-exponential factor for the reaction.
- E_a is the activation energy for the reaction (J/mol).
- R is the gas constant: 8.3145 (J/mol·K).
- T is the temperature (K).

The pre-exponential factor, is a constant that can be derived experimentally or numerically. It is also called the frequency factor and describes how often two molecules collide. To first approximation, the pre-exponential factor is considered constant [43].

The activation energy, represents the mínimum energy requirement that must be met for a chemical reaction to occur. Every molecule possess a certain minimum amount of energy. When these molecules come into contact, the kinetic energy of the molecules can be used to stretch, bend, and ultimately break bonds, leading to chemical reactions. If molecules move too slowly with little kinetic energy lacking sufficient kinetic energy, or if they meet at an unfavorable angle they do not react and simply bounce off each other. However, when molecules approach with adequate speed and the correct orientation, such that their combined kinetic energy surpasses the activation energy barrier, a chemical reaction ensues [43].

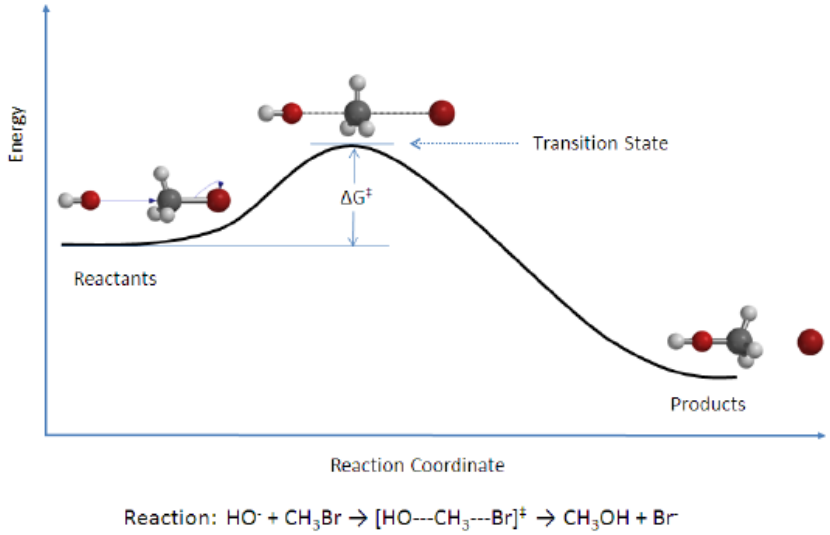

Figure 2. Reaction coordinate diagram [60].

The activation energy, denoted as $\Delta G^{\ddagger}$ in Figure 2, is the energy difference between the reactants and the activated complex, often referred to as the transition state. In a chemical reaction, the transition state is defined as the highest-energy state of the system. When molecules from the reactants collide with enough kinetic energy exceeding that of the transition state, they initiate a reaction, leading to the formation of products. In other words, the higher the activation energy, the harder it is for a reaction to occur and vice versa [43].

2.2. COMPLEX REACTIONS

The kinetics of complex reactions refers to the study of the reaction rate and mechanism of chemical reactions that involve multiple elementary steps [44]. These reactions are characterized by a series of multiple reaction stages, transient intermediates, parallel reactions, or any combination of these factors between the reactants and the final products. In general, they are divided into two categories: chain reactions and step reactions.

In chain reactions, an initial step, known as initiation, generates reactive species that then propagate and are consumed in a series of reactions. These reactions can include elementary

addition, elimination, or substitution reactions, depending on the reactants and products involved. Finally, the reaction has a termination step, where the reactive species combine or deactivate.

Step reactions involve multiple elementary steps that occur in parallel or in sequence. Each step can have its own reaction rate and may involve the formation or breaking of chemical bonds. These steps can be reversible or irreversible.

Compared to simple kinetics, the rate of a reaction cannot be described as a general equation for all complex reactions because each of them has specific conditions that have to be present in the rate equation.

2.2.1. LG-MgO dissolution reaction

LG-MgO is primarily composed of MgO about a 50% [39,45]. For this reason, the kinetics revolve around the dissolution properties of MgO.

MgO is almost insolubility in water due to the presence of intramolecular forces that water cannot overcome, i.e., it dissolves to a limited extent [54]. The surface of MgO undergoes hydration, converting the magnesium oxide into magnesium hydroxide. Subsequently, when magnesium hydroxide is dissolved in water, it dissociates into magnesium ions (Mg^{2+}) and hydroxide ions (OH^-). The described process is shown in Equations 6 and 7.

$$MgO_{(s)} + H_2O_{(aq)} \rightleftarrows Mg(OH)_{2\,(aq)} \quad \text{(Eq. 6)}$$

$$Mg(OH)_{2\,(aq)} \rightleftarrows Mg^{2+}_{(aq)} + 2\,OH^-_{(aq)} \quad \text{(Eq. 7)}$$

However, MgO can be dissolved in acidic solutions due to the reaction with acid.

Park et al. [46] showed that the dissolution behavior of powdered magnesium oxide is quite similar to that of magnesium hydroxide. This led them to conclude that the magnesium oxide surface is rapidly converted to hydroxide, which later reacts with hydrogen ions in the dissolution reaction. Altough the described reaction involves different simple reactions, the mechanism is shown in Equation 8.

$$MgO_{(s)} + H^+_{(aq)} \rightleftarrows Mg^{2+}_{(aq)} + OH^-_{(aq)} \quad \text{(Eq. 8)}$$

Equations 6, 7, and 8 are equilibrium reactions. This phenomenon arises from the equilibrium state between the solid reactant and the Mg^{2+} and OH^- species in the medium. As the medium

pH reaches the equilibrium pH, the amount of dissolved magnesium ions decreases due to the equilibrium formed in the system. Considering the MgO K_{sp}, the equilibrium pH is about 10.3 [47]. Due the fact that the kinetics revolve around equilibrium reactions, equilibrium reactions are explained in the following subsection.

2.2.2. Reversible reactions

In reversible reactions, the extent of the reaction is limited by the fact that the reactants transformed by the forward reaction are, as the reaction proceeds, regenerated in proportion by the reverse reaction. After a certain amount of time, the rates of the forward and reverse reactions become equal. At this point, an equilibrium state has been reached [48].

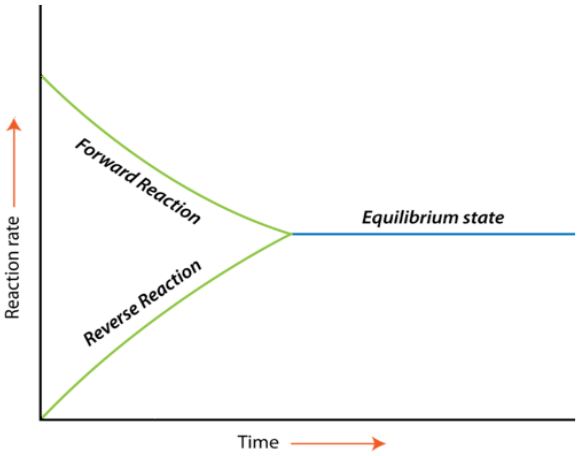

Figure 3. A visual representation of the variation in reaction rate versus time for a reaction involving: Rectant A + Reactant B ⇄ 2 Product P [49].

Chemical equilibrium is a dynamic process. The forward and reverse reactions continue to occur even after equilibrium has been reached. However, because the rates of the reactions are the same, there is no change in the relative concentrations of reactants and products for a reaction that is at equilibrium [49].

Equilibrium state can be achieved in various ways: it can result from the opposition of reactions of the same order (whole or fractional), reactions of different orders, or even the

opposition of reactions that do not follow any order [48]. In this study, the reversible reactions that result from the opposition of reactions are considered to exhibit a certain order. An equilibrium reaction can be symbolized in the form:

$$v_A A + v_B B \rightleftarrows v_M M + v_N N \quad \text{(Eq. 9)}$$

where:

- v_A, v_B, v_M, and v_N are the stoichiometric coefficients.
- A and B are the reactants.
- M and N are the products.

The reaction rate from direct (v_D) and inverse (v_I) reaction is represented in Equation 10, according with the consideration made before (both reactions follow a specific order):

$$v_D = k_D [A]^{\alpha} [B]^{\beta} \quad v_I = k_I [M]^m [N]^n \quad \text{(Eq. 10)}$$

where:

- k_D is the direct reaction rate constant (units depend on the fractional parameters).
- k_I is the inverse reaction rate constant (units depend on the fractional parameters).
- [A], [B], [M], [N] are the concentrations of reactants and products (mol/volume).
- α, β, m, and n are the fractional parameters.

The general rate reaction from the direct reaction is the difference between the direct reaction rate and the inverse reaction rate:

$$r = r_D - r_I = (1/v_A) \cdot (d[A]/dt) = k_D [A]^{\alpha} [B]^{\beta} - k_I [C]^{\lambda} [D]^{\mu} \quad \text{(Eq. 11)}$$

where:

- r is the general reaction rate (mol/(L·min)).
- r_D is the direct reaction rate (mol/(L·min)).
- r_I is the inverse reaction rate (mol/(L·min)).
- d[A]/dt is the reaction rate where A is being consumed to form C and D.

Once the system reaches equilibrium, the direct and inverse reaction rates have the same value, resulting in a net reaction rate of 0. By combining the resulting net rate with Equation 11, Equation 12 is formed:

$$0 = r = r_D - r_I \rightarrow ([M]^m_{eq.} \cdot [N]^n_{eq.}) / ([A]^\alpha_{eq.} \cdot [B]^\beta_{eq.}) = k_D / k_I = K_c \quad \text{(Eq. 12)}$$

where:

- Kc is the equilibrium constant.

The rate expression is written as a product of a temperature-dependent term and a composition dependent term where the temperature-dependent term is represented by the reaction rate constant (k). In equilibrium reactions, the Arrhenius Law is fulfilled for the direct and the inverse reaction. Equations 13 and 14 show the Arrehnius Law for a reversible reaction.

$$k_D = A_D \cdot \exp(-E_{a,D}/RT) \quad \text{(Eq. 13)}$$

$$k_I = A_I \cdot \exp(-E_{a,I}/RT) \quad \text{(Eq. 14)}$$

where:

- A_D is the pre-exponential factor for the direct reaction.
- A_I is the pre-exponential factor for the inverse reaction.
- $E_{a,D}$ is the activation energy for the direct reaction (J/mmol).
- $E_{a,I}$ is the activation energy for the inverse reaction (J/mmol).
- R is the gas constant: $8.3145 \cdot 10^{-3}$ (J/mmol·K).
- T is the temperature (K).

3. OBJECTIVES

The main objective of this study is to investigate the dissolution kinetic behavior of LG-MgO, a magnesium-rich industrial by-product suitable for struvite precipitation. The dissolution kinetic behaviour was studied in an acidic medium and a neutral medium. To meet this main objective, the following specific objectives were planned:

- Investigate the dissolution of Mg^{2+} of the LG-Mg in an acidic medium. Analyze the effect of temperature and the initial LG-MgO concentration on the dissolution kinetics and identify any trends or correlations.

- Study the dissolution of Mg^{2+} of the LG-MgO in a neutral medium. Compare the dissolution rates in the neutral medium with those obtained in the acidic medium.

- Explore the influence of temperature on the dissolution kinetics of LG-MgO and determine the activation energy associated with the dissolution process. Perform dissolution experiments at different temperatures within a defined range (15, 25, 35, 45 and 55 ºC), both in the acidic and neutral media.

- Find the kinetic values that will enable the proposed kinetic study to accurately describe the amount of magnesium ions that dissolve in the medium.

By accomplishing these specific objectives, this research paves the path for optimizing LG-MgO dosage to facilitate struvite precipitation and minimize magnesium losses through the effluent. Future research and applications can utilize this knowledge to determine the amount of LG-MgO that needs to be dosed in the medium and its dissolution behaviour.

4. MATERIALS AND METHODS

4.1. MEDIUM PREPARATION

4.1.1. Neutral medium

The dissolution experiments of LG-MgO in a medium without buffer solution where carried out in deionized water.

4.1.2. Acidic medium

The acidic medium was chosen as wastewater presents buffer capacity able to react with the released OH^- (NH_4^+, HCO_3^- and $H_2PO_4^-$). Therefore, the experiments aimed to estimate the amount of magnesium dissolved when LG-MgO is added in wastewater.

The medium used consists of a buffer solution containing citric acid. Citric acid is a triprotic acid with pK_a values of 3.128, 4.761, and 6.369 at 25 ºC [50]. The initial pH for the acidic medium had approximately the value of 6.369. This choice was made because the ionic chromatograph used to measure the concentration of magnesium ions does not provide accurate readings at low pH values.

To prepare the acidic medium, different solutions were created as follows:

- A 1.5 M citric acid solution was prepared by using deionized water and citric acid anhydrous.
- A 2 M solution of NaOH was prepared by using deionized water and sodium hydroxide pellets, extra pure, from Scharlab S.L.

Next, 6.2 L of deionized water were mixed with 93 mL of the 1.5 citric acid solution. Subsequently, 170 mL of the NaOH solution was added to the mixture to achieve the buffer pH.

4.2. LG-MGO COMPOSITION

The LG-MgO industrial by-product used to develop the dissolution kinetic model was provided by Magnesitas Navarras, S.A (Navarra, Spain). The mineral composition of the LG-MgO used in this study was provided by Magnesitas Navarras, S.A (Table 1).

Table 1. Mineral composition of LG-MgO.

	Units	
MgO	%	46.14
CaO	%	-
SiO_2	%	2.13
$Mg(OH)_2$	%	2.89
$MgCO_3$	%	21.71
$CaMg(CO_3)_2$	%	5.67
$CaCO_3$	%	10.37
$MgSO_4$	%	3.20
$CaSO_4$	%	3.11
Others	%	3.17

4.3. LG-MGO COMPONENTS DISSOLUTION PROPERTIES

As shown in Table 1, the substances that contain magnesium of LG-MgO are MgO, $Mg(OH)_2$, $MgCO_3$, $CaMg(CO_3)_2$, and $MgSO_4$. Although MgO is the main component, the properties of the other compounds are the following:

$Mg(OH)_2$ (magnesium hydroxide) is soluble in water. It has a low solubility, but it does dissolve to a small extent in water, forming magnesium ions (Mg^{2+}) and hydroxide ions (OH^-). The dissolved ion concentration increases with decreasing pH due to equilibrium formed at pH around 10.3.

$MgCO_3$ (magnesium carbonate o magnesite) and **$CaMg(CO_3)_2$** (dolomite) are both partly soluble in water. They do not easily dissolve in water, and their solubility is generally low because they present intramolecular forces that water cannot overcome. However, they can dissolve to some extent in acidic solutions due to the reaction with acid.

$MgSO_4$ (magnesium sulfate) is soluble in water and acid, dissociating into magnesium ions (Mg^{2+}) and sulfate ions (SO_4^{2-}).

For these reasons, the results in an acidic medium are expected to have a higher magnesium ions concentration than in neutral conditions.

4.4. EXPERIMENTAL SET-UP

4.4.1. Experimental device

The experimental device used consists of two closed jacketed reactors with stirring connected to a thermal bath (Figure 4). Two reactors were used to duplicate to verify the accuracy of the experimental results.

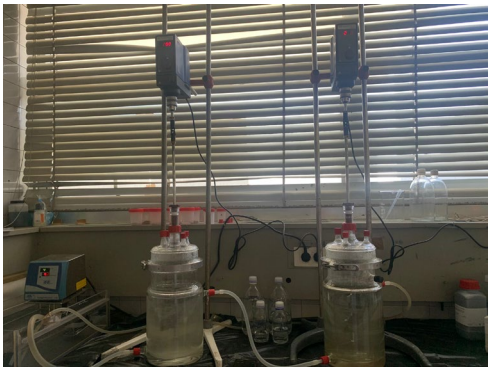

Figure 4. Experimental device.

4.4.2 Experimental procedure

In two reactors two liters of deionized water or acidic solution were introduced. Afterward, the thermal bath was connected, and the temperature value was set (15, 25, 35, 45 or 55 ºC). Stirring was then connected to ensure that the medium reached the targeted temperature. Next, the selected amount of LG-MgO was introduced into both reactors. Once all the LG-MgO was in reactors, the timer was started. From this point, at 5, 10, 15, 20, 25, 30, 40, 50, and 60 minutes, 10 mL of the solution were withdrawn from both reactors. These samples were immediately filtered using a 0.22 µm regenerated cellulose syringe filter, and the pH of each sample was measured afterward. Finally, the samples were diluted and duplicated for analysis. Once each sample was analyzed, the dissolved Mg^{2+} concentration was obtained.

4.4.3. Experiments

30 experiments were carried out in this research. A duplicate of each experiment was carried out to verify the accuracy of the results. Table 2 shows the experimental conditions of each experiment.

Table 2. Conditions of the experiments carried out in this research.

Experiment	LG-MgO concentration added (mmol/L)	Temperature (ºC)	Medium
1	3.875	15	Neutral
2	3.875	25	Neutral
3	3.875	35	Neutral
4	3.875	45	Neutral
5	3.875	55	Neutral
6	3.875	15	Acidic
7	3.875	25	Acidic
8	3.875	35	Acidic
9	3.875	45	Acidic
10	3.875	55	Acidic
11	5.812	15	Neutral
12	5.812	25	Neutral
13	5.812	35	Neutral
14	5.812	45	Neutral
15	5.812	55	Neutral
16	5.812	15	Acidic
17	5.812	25	Acidic
18	5.812	35	Acidic
19	5.812	45	Acidic
20	5.812	55	Acidic
21	7.750	15	Neutral
22	7.750	25	Neutral
23	7.750	35	Neutral
24	7.750	45	Neutral
25	7.750	55	Neutral
26	7.750	15	Acidic
27	7.750	25	Acidic
28	7.750	35	Acidic
29	7.750	45	Acidic
30	7.750	55	Acidic

The results of the LG-MgO dissolution in neutral medium at temperatures of 45 and 55°C are not shown due to an error in the sample analysis.

4.5. ANALYTICAL METHODS

Mg^{2+} was analyzed using an 861 Advanced Compact IC Metrohm ionic chromatographer equipped with Metrosep C 4-150/4.0 column and following manufacturer's protocol (Figure 5). Before ion analysis, the samples were filtered through a 0.22 µm regenerated cellulose syringe filter. pH was measured using MultiMeter MM41 (Crison) equipped with a pH electrode (Crison, 50 52) (Figure 6).

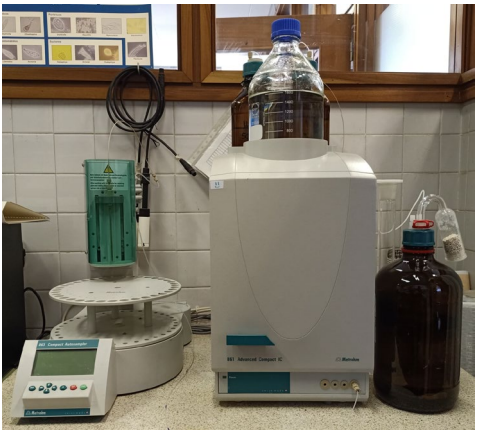

Figure 5. Advanced Compact IC Metrohm ionic chromatographer.

Figure 6. MultiMeter MM41 (Crison).

4.6. KINETICS DISSOLUTION MODELING

In the neutral medium experiments, it was observed that when 0.15 to 0.7 mg/L of MgO were dosed, an equilibrium pH was achieved. However, dosing the same amount of MgO into acid the equilibrium pH was not reached. For these reasons, the reaction and the kinetic used in a neutral medium considers the dissolution reaction as an equilibrium reaction, while the reaction and the kinetic used in the acidic medium considers the dissolution reaction as a simple reaction due to the excess of H^+ ions.

4.6.1. Neutral medium model description

Considering the system as a reversible reaction where the molar relation is 1:1, the dissolution reaction is:

$$A\ (\text{dissolution}) \rightleftarrows B\ (\text{precipitation}) \quad \text{(Eq. 15)}$$

where:

- A are magnesium ions undissolved.
- B are magnesium ions dissolved.

The proposed model, based on Quintana et al. [44], applies a first-order kinetic model. This model relates the dissolution rate (r_A) to the rate constant (k) and the reactant concentration at time t (C_A) minus the reactant concentration at equilibrim (C_e). The proposed kinetic model can be expressed as follows:

$$-(dC_A/dt) = r_A = k \cdot (C_A - C_e) \quad \text{(Eq. 16)}$$

By integrating Equation 16, the following equation was obtained:

$$-\ln((C_A - C_e) / (C_0 - C_e)) = k \cdot (t - t_0) \quad \text{(Eq. 17)}$$

where:

- C_0 is the initial concentration of undissolved magnesium (mmol/L).
- t_0 is the initial time (min).

Ordering the terms found in Equation 17, isolating C_A and considering t_0 equals to 0 min, Equation 17 can be represented as follows:

$$C_A = C_e - (C_0 - C_e) \cdot e^{k \cdot t} \text{ (Eq. 18)}$$

4.6.2. Acidic medium model description

Considering the system as a forward reaction where the molar relation is 1:1, the dissolution kinetics can be represented as follows:

$$A \rightarrow B \text{ (Eq. 19)}$$

where:

- A are magnesium ions undissolved.
- B are magnesium ions dissolved.

The proposed model consists in a alfa order model that assumes that the dissolution rate depends on the concentration of the undissolved magnesium ions raised to a fractional parameter (α). The proposed kinetic model can be expressed as follows:

$$-(dC_A/dt) = r_A = k \cdot (C_A)^{\alpha} \text{ (Eq. 20)}$$

where:

- r_A is the dissolution rate at which the magnesium ions dissolve (mmol/min).
- k is the dissolution rate constant.
- C_A is the magnesium ions concentration that did not dissolve at a specific time (mmol/L).
- α is the fractional parameter.

By integrating Equation 20, the following equation was obtained:

$$((C_A^{-\alpha+1} - C_0^{-\alpha+1}) / -\alpha+1) = k \cdot (t - t_0) \text{ (Eq. 21)}$$

where:

- C_0 is the initial concentration of undissolved magnesium (mmol/L).
- t_0 is the initial time (min).

Ordering the terms found in Equation 17, isolating C_A and considering t_0 equals to 0 min, Equation 21 can be represented as follows:

$$C_A = (C_0^{-\alpha+1} - k\, t\, (-\alpha+1))^{1/-\alpha+1} \quad \text{(Eq. 22)}$$

4.6.3. Parameter determination using the minimum sum of squared difference

To determine the values of the different kinetic parameters such as E_a, A, k and α for both models, a parameter estimation process was carried out. The minimum sum of squared difference approach was used, comparing the experimental concentrations of undissolved magnesium results with the model predictions.

The experimental value of C_A and C_0 for both models was obtained experimentally using the Advanced Compact IC Metrohm ionic chromatographer.

The predicted value of C_A using both model was calculated following the next steps:

1. Arrhenius equation (Equation 5) has been employed to estimate the activation energy (E_a) and pre-exponential factor (A). By giving a random number to those two parameters, a value of k was calculated for each temperature and models.
2. The value of C_e used for the neutral medium model was the value of C_A obtained at time equal to 60 min. For each temperature and initial concentration, a different value of C_e was used.
3. A random number was given to α.

Combaining all of these steps, and using Equations 18 and 22, a number of C_A is obtained. Once obtained, the minimum sum of squared difference was used.

5. RESULTS AND DISCUSSION

5.1. DISSOLUTION OF LG-MGO IN NEUTRAL MEDIUM

Figure 7 depict the variation in undissolved magnesium ion concentration in the LG-MgO over time in neutral medium. The resulds showed that the concentrations of magnesium ions dissolved at 15, 25 and 35 ºC are around 0.72, 0.85 and 0.95 mmol/L respectively, regardless of the concentration of LG-MgO added. Furthermore, for durations exceeding 40 minutes, the undissolved magnesium ion concentration remained nearly constant for all temperatures. Also, the results indicate an increase in the dissolved concentration as the temperature increases.

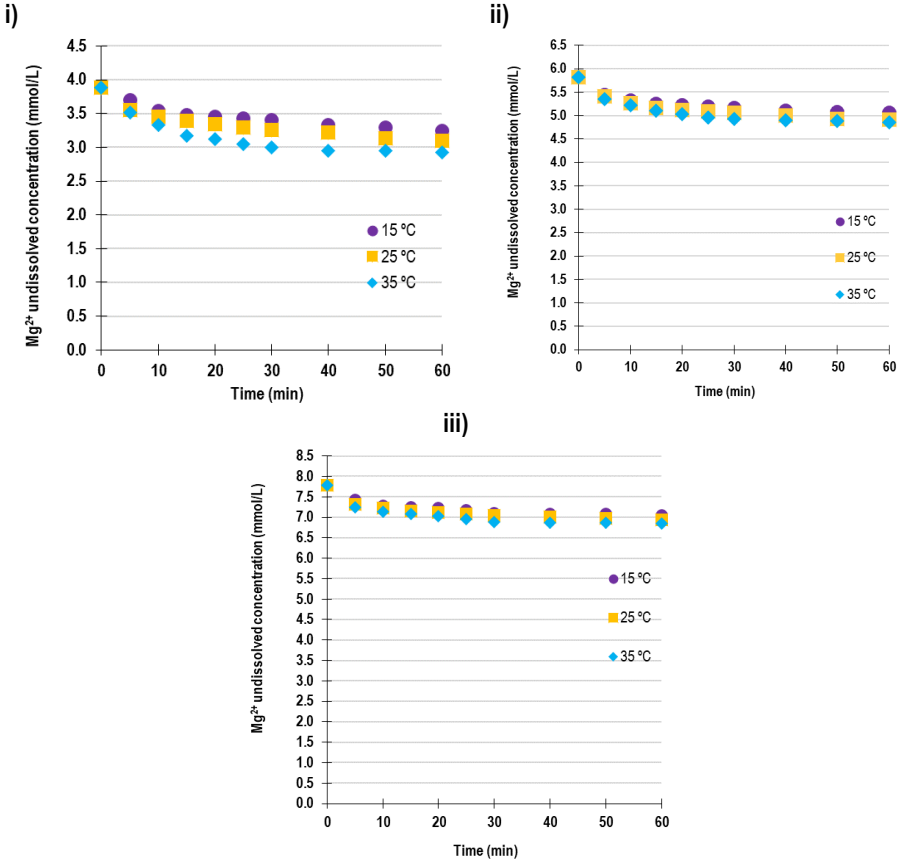

Figure 7. Variation of undissolved magnesium concentration over time in neutral medium. Initial concentration of LG-MgO (i) 0.25 mg/L, (ii) 0.375 mg/L, (iii) 0.5 mg/L

Figure 8 illustrates the pH changes over time when LG-MgO is added to neutral medium. The pH behaviour follows a logarithmic trend. In first minutes there was a rapid increase in pH, then the pH stabilized around 10.9 to 11.0 in all experiments, close to the MgO acid-base equilibrium pH.

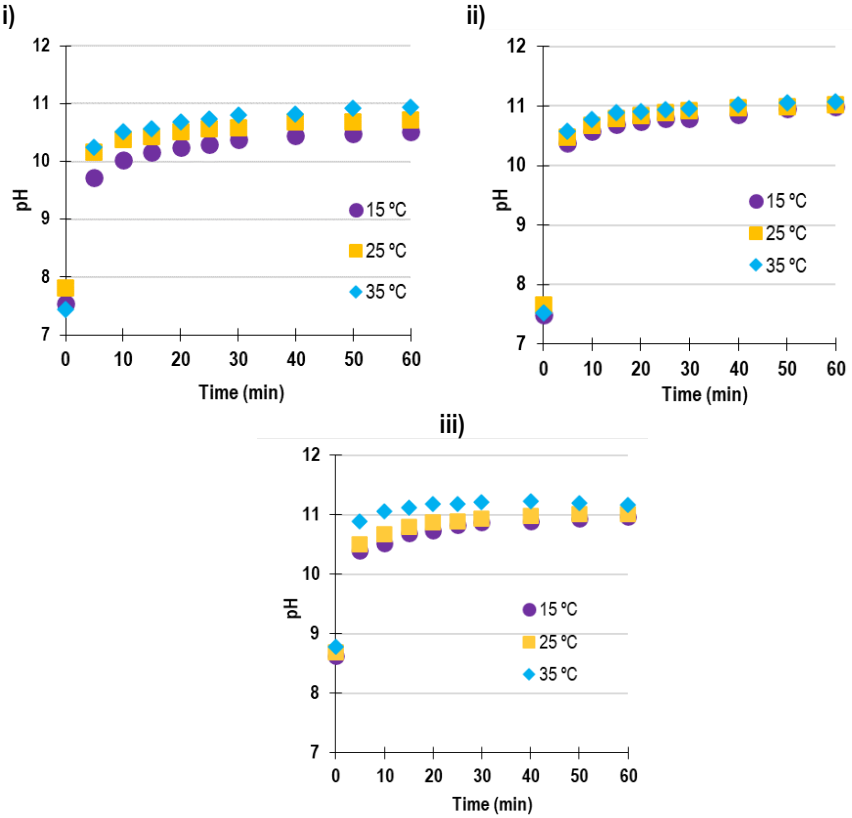

Figure 8. Variation of pH over time in neutral medium.
Initial concentration of LG-MgO (i) 0.25 mg/L, (ii) 0.375 mg/L, (iii) 0.5 mg/L

The behavior of the dissolution of the Mg ion from LG-MgO and the pH follows the same trend. The dissolution reaction of MgO produces OH^- ions (as illustrated in Equations 6 and 7). Consequently, as more magnesium dissolves (less magnesium in the LG-MgO), the pH value increases. This can be observed in the initial 40 min. Afterwards, both the magnesium dissolution and pH decrease. The dissolution of magnesium and the pH are constrained by the proximity to the equilibrium of MgO.

The percentage of undissolved magnesium ions was estimated by dividing the difference between the concentrations at time 0 and 60 by the concentration at time 0 (referenced in Table 1). The outcomes of this calculation are presented in Table 3.

Table 3. Percentatge of undissolved magnesium carried out in neutral medium.

Undissolved magnesium (%)			
LG-MgO mass (g)	**Temperature (ºC)**		
	15	**25**	**35**
0.5	82.9	79.7	75.3
0.75	86.9	84.4	83.4
1.0	90.6	89.2	88.1

As illustrated in Figures 7 and 8, along with Table 3, an increase in temperature correlates with a decrease in Mg^{2+} concentration and a corresponding rise in pH across all experiments. Higher temperatures privde higher kinetic energy to the particles, accelerating their movement and enhancing the likelihood of collisions and reactions [55]. Consequently, a more rapid dissolution occurs upon contact with water, resulting in increased magnesium dissolution. This clarifies why the percentage of undissolved magnesium decreases as the temperature increased from 15 to 35 °C (Table 3). These results show that the equilibrium constant is temperature-dependent. As noted above, after 40 minutes the Mg concentration in the LG-MgO and pH varies little, therefore, the magnesium concentration at 60 minutes was considered to be the equilibrium concentration. In all experiments, fluctuations in this parameter were evident with changing temperatures, with values increasing as temperature increased. This suggests that the equilibrium constant (K_{eq}), the parameter linking the concentrations of reactants and products at equilibrium under specific conditions, increases as the temperature increases. Applying the Van't Hoff equation, which correlates changes in the equilibrium constant of a reaction with temperature variations based on the standard enthalpy change (ΔH), and Le Chatelier's principle, which proposes that a system at equilibrium adjusts in response to external disturbances, reveals that the dissolution of magnesium ions is an endothermic process.

5.2. DISSOLUTION OF LG-MGO IN ACIDIC SOLUTION

Figure 9 depicts the variation in undissolved magnesium ion concentrations in the LG-MgO in an acidic solution over time. Exponential curves were observed in all experiments. This results in a swift decrease in magnesium ion concentration within the initial 10 minutes, with this effect being more pronounced at higher temperatures. After 40 minutes, the concentration of undissolved magnesium ions in all experiments remained nearly constant. Additionally, an increase in the initial concentration of LG-MgO led to a reduced concentration of undissolved magnesium ions.

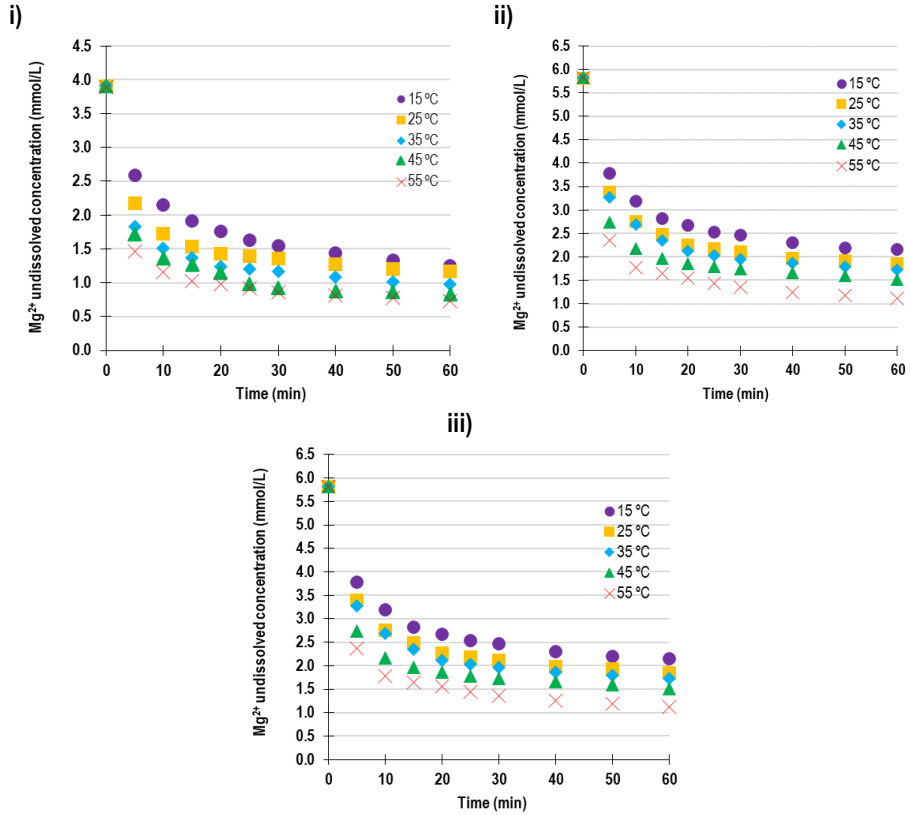

Figure 9. Representation of predictions from the kinetic model observed in neutral medium. Initial concentration of LG-MgO (i) 0.25 mg/L, (ii) 0.375 mg/L, (iii) 0.5 mg/L

Figure 10 illustrates the pH variations over time when LG-MgO is introduced into an acidic medium. All experiments showed a rapid rise in pH within the first 5 minutes, with this effect being more pronounced at higher temperatures. Additionally, there was a notable discrepancy in pH values between experiments. Specifically, while the pH remains relatively consistent throughout the entirety of the experiment in Figure 10 (i), (ii) and (iii) display an upward trend in pH values from 0 to 30 minutes. Subsequently, the pH stabilizes and remains nearly constant.

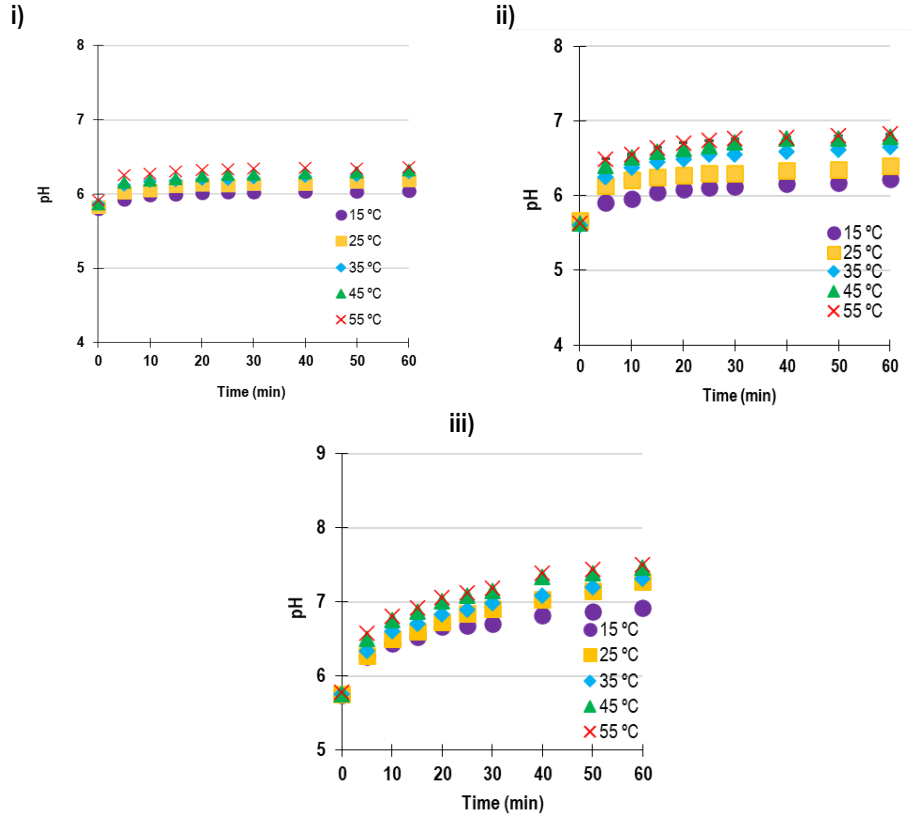

Figure 10. Variation of pH over time in acidic medium.
Initial concentration of LG-MgO (i) 0.25 mg/L, (ii) 0.375 mg/L, (iii) 0.5 mg/L

The rapid decrease in concentration suggests that LG-MgO exhibits high reactivity upon initial contact with an acid solution. However, this reactivity diminishes after a certain period, typically after 10 minutes. LG-MgO primarily comprises MgO, which reacts with H^+ (Equation 8). The excess of protons promotes the dissolution of MgO. This acid solution incorporates a meticulously selected citric acid buffer solution designed to counteract pH increases and maintain a consistent

pH level throughout the experiment. Consequently, there minimal pH fluctuation were observed during the experiment. After first 30 minutes, the concentration of undissolved magnesium ions remained stable in all experiments. To elucidate this behavior, the percentage (%) of undissolved magnesium ions was estimated. The outcomes of these calculations are presented in Table 4.

Table 4. Percentatge of undissolved magnesium carried out in acidic medium.

Undissolved magnesium (%)					
LG-MgO mass (g)	**Temperature (ºC)**				
	15	**25**	**35**	**45**	**55**
0.5	32.1	30.0	25.0	21.3	18.6
0.75	37.0	31.9	29.7	26.0	19.1
1.0	37.4	29.9	26.7	24.1	23.7

Table 3 shows that the reaction remains incomplete due to the presence of unreacted magnesium. LG-MgO is a by-product comprising various components. When this particle interacts with acid, its constituents (such as MgO, MgOH, and $MgSO_4$) increase their solubility when dissolved in acidic media as shown in this section,resulting in the dissolution of a substantial portion of magnesium within a shorter timeframe. Conversely, components like $MgCO_3$ react with the acid to a lesser extent and require more time to dissolve a significant amount of magnesium. This elucidates why the concentration of undissolved magnesium ions stabilizes in all experiments after 30 minutes (Figure 9). These experimental results imply that more extended durations are requisite to completely dissolve a higher percentage of magnesium due to the slower reaction rates of certain magnesium components. Experimental results also show that temperature exerts a notable influence on LG-MgO dissolution in acid media. As depicted in Figure 9 as well as Table 4, the concentration consistently diminishes across all experiments with increasing temperatures. As explained in Section 5.1, higher temperatures provide higher kinetic energy to the particles, enhancing their mobility and collision frequency, thereby accelerating reactions.

5.3. LG-MGO DISSOLUTION KINETICS

5.3.1. LG-MgO dissolution kinetics in neutral medium

The kinetic parameters were obtained by minimizing the sum of squared differences, where it was aimed for the concentrations obtained by the model using Equation 18 to align with the experimental concentrations. Figure 11, illustrates the kinetic model predictions alongside the experimental values over time.

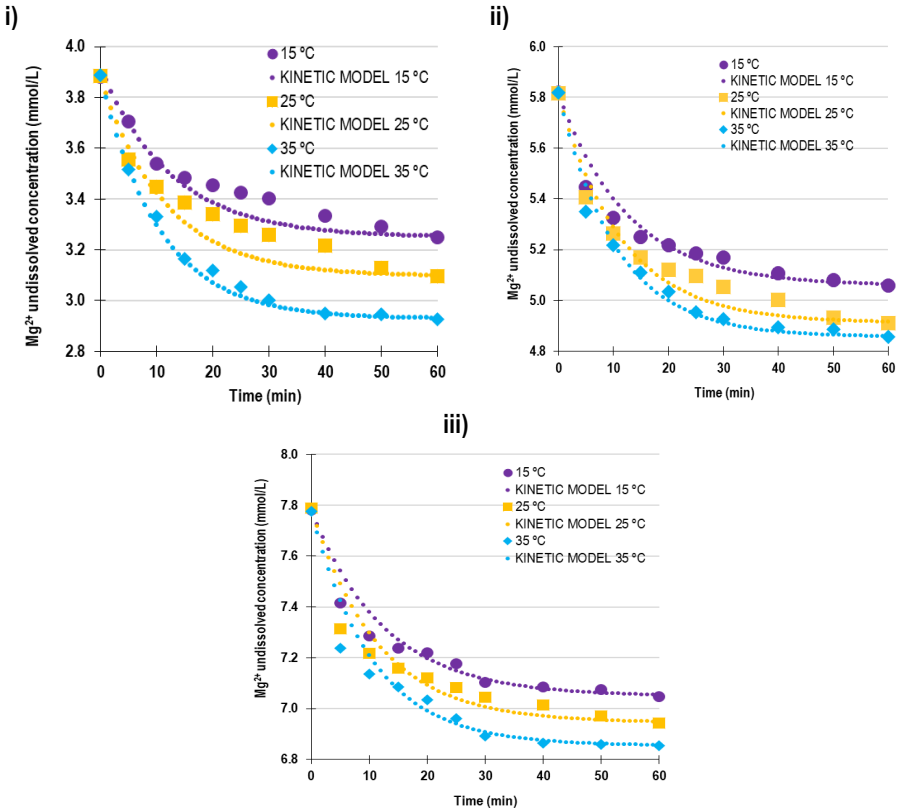

Figure 11. Representation of predictions from the kinetic model observed in neutral medium. Initial concentration of LG-MgO (i) 0.25 mg/L, (ii) 0.375 mg/L, (iii) 0.5 mg/L

Figure 11 shows the concentrations predicted by the kinetic model and the experimental concentrations. It can be seen that the kinetic model adjusts better as the temperature and time increase. Although the graphical representations suggest the model's effectiveness, a definitive confirmation remains elusive. To validate the kinetic model, a residual plot was constructed. This

plot graphically illustrates residuals or errors on the vertical axis against the independent variable (or predicted values) on the horizontal axis. Figure 12 display the residual plots corresponding to each initial concentration of LG-MgO. Within each plot, a linear regression was executed to ascertain the model's accuracy.

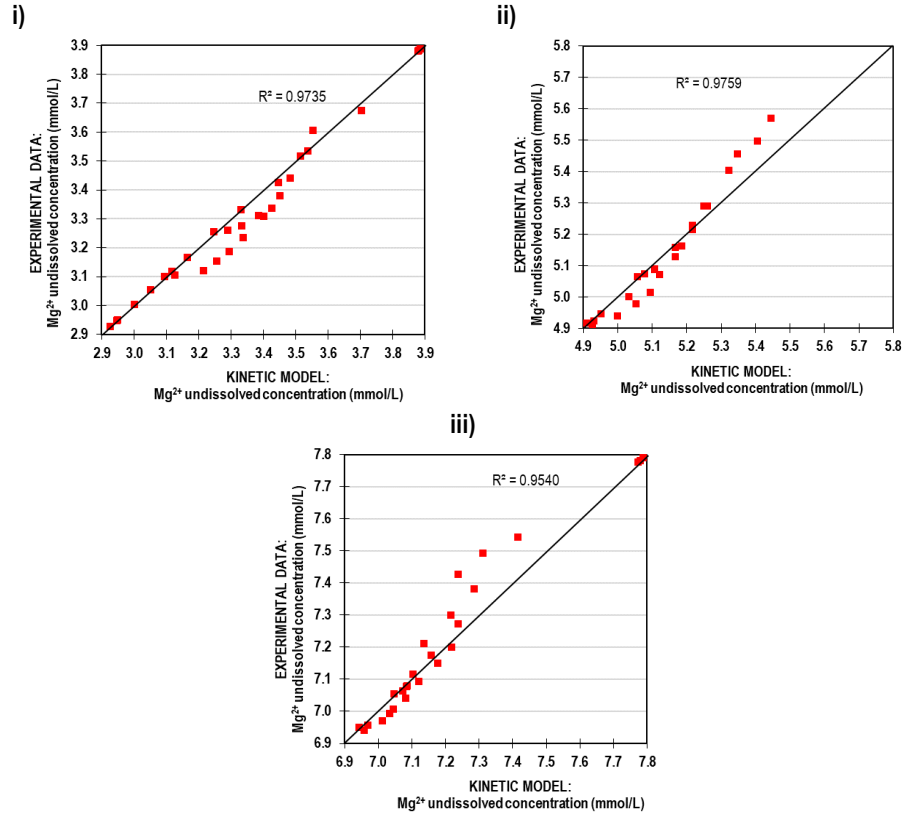

Figure 12. Residual plot for the kinetic model in neutral medium.
Initial concentration of LG-MgO (i) 0.25 mg/L, (ii) 0.375 mg/L, (iii) 0.5 mg/L

Upon examining the R^2 values presented in Figure 12, it can be inferred that the proposed first-order kinetic model predictions approach the experimental values. Furthermore, R^2 indicates that the proposed model could be modified to achive an R^2 higher than 0.99. Despite that, it can be concluded that the first-order kinetic model effectively predicts the variaton of concentration over time (up to 60 minutes) within temperatures ranging from approximately 15°C to 35°C in a neutral medium.

Subsequently, Table 5 displays the values of the kinetic parameters utilized to formulate this model.

Table 5. Kinetic parameters for neutral medium.

Kinetic parameters	
Ea (J/mmol)	6.72
A (mmol/L·min)	1.31
k values for each temperature (mmol/(L ·min))	
15 ºC	$7.92 \cdot 10^{-2}$
25 ºC	$8.70 \cdot 10^{-2}$
35 ºC	$9.50 \cdot 10^{-2}$

Observing Table 5, an increase in the value of the reaction constant is accompanied by a decrease in the equilibrium concentration as the temperature rises.

5.3.2. LG-MgO dissolution kinetics in acidic medium

The kinetic parameters were obtained by minimizing the sum of squared differences, where it was aimed for the concentrations obtained by the model using Equation 22 to align with the experimental concentrations. Figure 13, illustrates the kinetic model predictions alongside the experimental values over time.

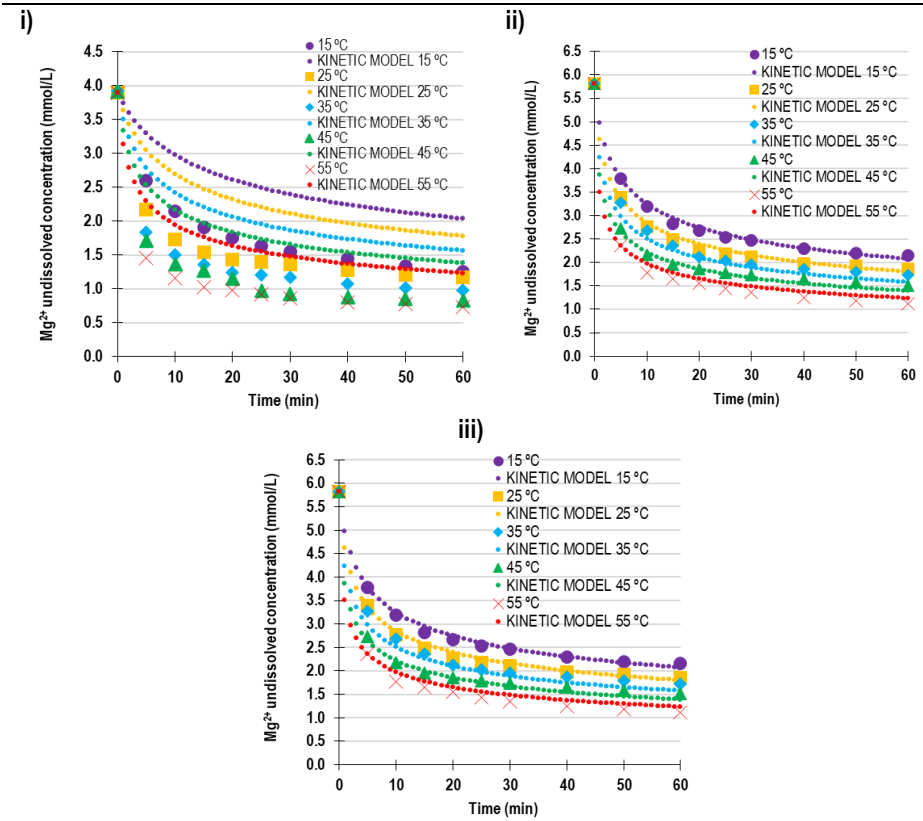

Figure 13. Representation of predictions from the kinetic model observed in acidic medium. Initial concentration of LG-MgO (i) 0.25 mg/L, (ii) 0.375 mg/L, (iii) 0.5 mg/L

Upon completing the minimization of the sum of squared differences, values for the predicted kinetic model were derived from Equation 22. To validate this model against experimental values, calculations based on the kinetic model were graphically represented in Figure 13. It is evident that the predicted values closely align with the experimental values when the initial mass of LG-MgO is 0.75 g. However, for the other two cases, the trend is similar although the experimental values and predicted values diverges. To conclusively interpret these observations, a residual plot was developed for each experiment. Figure 14 presents the residual plots corresponding to each initial concentration of LG-MgO. Within each plot, a linear regression was conducted to determine the model's accuracy, and consequently, the R^2 value has been included in each plot.

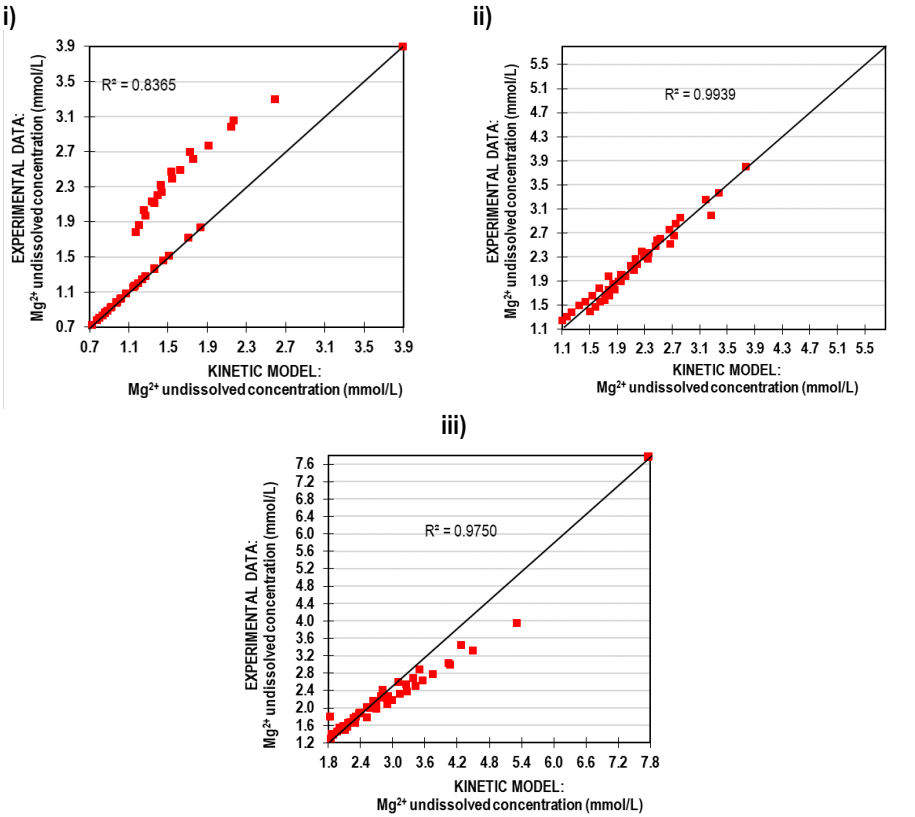

Figure 14. Residual plot for the kinetic model in acidic medium.
Initial concentration of LG-MgO (i) 0.25 mg/L, (ii) 0.375 mg/L, (iii) 0.5 mg/L

As observed, the model predictions closely match the experimental variations in the concentration of undissolved magnesium ions when the initial concentration of LG-MgO is 0.375 mg/L. However, this alignment diminishes when the initial concentration of LG-MgO varies.

Considering the information presented above, one can infer that the proposed kinetic model tailored for acidic mediums does not accurately forecast the variation in the concentration of undissolved magnesium ions over time. However, the magnitude at which these values diverge seems to fluctuate based on the initial concentration of LG-MgO. This suggests that the initial equation employed for the kinetic model (Equation 20) may require an additional parameter representing the initial concentration. By integrating this parameter into the equation, it could potentially refine the model, addressing the observed discrepancies.

5.3. COMPARISON BETWEEN ACIDIC MEDIUM RESULTS AND NEUTRAL MEDIUM RESULTS

When comparing the previous results obtained from neutral and acidic media, the following conclusions can be drawn:

- It is evident that the quantity of dissolved magnesium is significantly greater in the acidic medium. This fact is exemplified by the data presented in Tables 3 and 4, which clearly demonstrate a considerably lower total concentration of undissolved magnesium in the acidic medium compared to the neutral medium. The reason for this disparity can be attributed to the equilibrium pH. While in the neutral medium this equilibrium is reached resulting in minimal magnesium dissolution, in the acidic medium no equilibrium is reached. Even more, LG-MgO exhibits a more pronounced dissolution reaction with acid as opposed to water. This happens due to the excess of protons in the acidic medium, which prevents reaching the equilibrium pH, allowing magnesium to continue dissolving. Consequently, the amount of magnesium that can be dissolved is higher in acid.

- For the neutral medium, kinetics were obtained from literature while for the acidic medium, semi-empirical kinetics was applied. The parameter estimates for each model showed a better prediction for the basic medium kinetics. This discrepancy can be attributed to the fact that the neutral medium accounted for equilibrium considerations. Equilibrium reactions are influenced by the equilibrium concentration, which is directly influenced by the temperature. Consequently, the proposed model for the acidic medium fails to accurately predict experimental values, indicating a potential dependency on the initial concentration that was not accounted for.

6. CONCLUSIONS

- The temperature exerts a notable influence on these experiments. An increase in temperature correlates with a decrease in concentration and a corresponding rise in pH (in neutral medium) across all experiments.

- LG-MgO is poorly soluble in neutral medium, resulting in minimal Mg dissolution. The solubility of MgO is limited by its pH. However, in acidic environments, the solubility of MgO increases as the equilibrium pH is not reached.

- In acidic medium not all of the Mg in the LG-MgO dissolved within 60 minutes. Furthermore, most of the dissolved Mg occurred in the first few minutes, after which the concentration of dissolved Mg decreased. When LG-MgO comes into contact with more reactive constituents, such as MgO, MgOH, and $MgSO_4$, they initiate faster reactions, leading to rapid dissolution. In contrast, components like $MgCO_3$ react with the acid to a lesser degree and necessitate more time to dissolve a substantial amount of magnesium. This suggests that more time is required to achieve a higher yield of dissolved magnesium.

- When LG-MgO dissolves in neutral medium, the MgO dissolves and reaches equilibrium. The first-order kinetic model effectively correlated the rate of phosphorus removal with its concentration. It was observed that as the temperature increased, there was a rise in the value of the reaction constant and a corresponding decrease in the equilibrium concentration.

- The proposed kinetic model designed for acidic mediums fails to accurately predict the variation in the concentration of undissolved magnesium ions over time. However, an alternative approach was proposed. The initial equation utilized for the kinetic model (Equation 20) requires the incorporation of an initial concentration parameter. By integrating this new parameter into the equation, it could potentially refine the model and address the discrepancies observed.

REFERENCES AND NOTES

1. European Commission (2023). https://ec.europa.eu/environment/natres/phosphorus.htm
2. Daneshgar, S.; Callegari, A.; Capodaglio, A.G.; Vaccari, D. The Potential Phosphorus Crisis: Resource Conservation and Possible Escape Technologies: A Review. *Resources* **2018**, 7, 37. https://doi.org/10.3390/resources7020037
3. European Sustainable Phosphorus Platform - Challenge: Geopolitics. (n.d.). https://phosphorusplatform.eu/links-and-resources/p-facts/p-fact-2
4. Kok, D.-J.D., Pande, S., van Lier, J.B., Ortigara, A.R.C., Savenije, H., Uhlenbrook, S., 2018. Global phosphorus recovery from wastewater for agricultural reuse. Hydrol. Earth Syst. Sci. 22, 5781–5799. https://doi.org/10.5194/hess-22-5781- 2018
5. Phosphate rock in EU Critical Raw Materials list (2014). https://phosphorusplatform.eu/scope-in-print/news/359-phosphate-rock-in-eu-critical-raw-materials-list
6. S. J.van Kauwenbergh, World Phosphate Rock Reserves and Resources, 2010.
7. Cho, R. (2019). Phosphorus: Essential to Life—Are We Running Out? State of the Planet. https://news.climate.columbia.edu/2013/04/01/phosphorus-essential-to-life-are-we-running-out/
8. European Commission Critical Raw Materials Resilience: Charting a Path towards Greater Security and Sustainability (2020).
9. van Dijk, K. C., Lesschen, J. P., & Oenema, O. (2016). Phosphorus flows and balances of the European Union Member States. The Science of the total environment, 542(Pt B), 1078–1093. https://doi.org/10.1016/j.scitotenv.2015.08.048
10. Cornel, P., & Schaum, C. (2009). Phosphorus recovery from wastewater: needs, technologies and costs. Water science and technology : a journal of the International Association on Water Pollution Research, 59(6), 1069–1076. https://doi.org/10.2166/wst.2009.045
11. Grady, C. P. L., Daigger, G. T., Love, N. G., & Filipe, C. D. M. (2011). Biological Wastewater Treatment. In CRC Press eBooks. https://doi.org/10.1201/b13775
12. European Commission. 2016. Eighth report on the implementation status and the programmes for implementation (as required by Article 17) of Council Directive 91/271/EEC concerning urban waste water treatment. http://eur-lex.europa.eu/legalcontent/en
13. J. T. Bunce, E. Ndam, I.D.Ofiteru, A. Moore, D.W. Graham Review of Phosphorus Removal Technologies and Their Applicability to Small-Scale Domestic Wastewater Treatment Systems Bunce et al. https://doi.org/10.3389/fenvs.2018.00008
14. The four stages of wastewater treatment plants (2022). https://www.idrica.com/blog/stages-of-wastewater-treatment-plants/

15. Kataki, S., West, H., Clarke, M., & Baruah, D. C. (2016). Phosphorus recovery as struvite from farm, municipal and industrial waste: Feedstock suitability, methods and pre-treatments. Waste management (New York, N.Y.), 49, 437–454. https://doi.org/10.1016/j.wasman.2016.01.003
16. Oleszkiewicz, J., Kruk, D. J., Devlin, T., Lashkarizadeh, M., and Yuan, Q. (2015). Options for Improved Nutrient Removal and Recovery from Municipal Wastewater in the Canadian Context. Winnipeg, MN: Canadian Water Network.
17. Muys, M., Phukan, R., Brader, G., Samad, A., Moretti, M., Haiden, B., Pluchon, S., Roest, K., Vlaeminck, S.E., Spiller, M., 2021. A systematic comparison of commercially produced struvite: Quantities, qualities and soil-maize phosphorus availability. Science of The Total Environment 756, 143726. https://doi.org/10.1016/j.scitotenv.2020.143726
18. Nguyen, T. T., Ngo, H. H., & Guo, W. (2013). Pilot scale study on a new membrane bioreactor hybrid system in municipal wastewater treatment. Bioresource technology, 141, 8–12. https://doi.org/10.1016/j.biortech.2013.03.125
19. Y. Comeau, K.J. Hall, R.E.W. Hancock, W.K. Oldham (1986). Biochemical model for enhanced biological phosphorus removal. https://doi.org/10.1016/0043-1354(86)90115-6.
20. Simon A. Parsons, Jennifer A. Smith; Phosphorus Removal and Recovery from Municipal Wastewaters. Elements 2008;; 4 (2): 109–112. https://doi.org/10.2113/GSELEMENTS.4.2.109
21. de-Bashan, L.E., Bashan, Y., 2004. Recent advances in removing phosphorus from wastewater and its future use as fertilizer (1997–2003). Water Research 38, 4222–4246. https://doi.org/10.1016/j.watres.2004.07.014
22. Siciliano, A.; Limonti, C.; Curcio, G.M.; Molinari, R. Advances in Struvite Precipitation Technologies for Nutrients Removal and Recovery from Aqueous Waste and Wastewater. Sustainability 2020, 12, 7538. https://doi.org/10.3390/su12187538
23. Relationship Between Solubility and Ksp (2022). https://chem.libretexts.org/Bookshelves/General_Chemistry/Map%3A_General_Chemistry_(Petrucci_et_al.)/18%3A_Solubility_and_Complex-Ion_Equilibria/18.2%3A_Relationship_Between_Solubility_and_Ksp
24. Jose Antonio Mejias, Andrew J Berry, Keith Refson, Donald G Fraser (1999). The kinetics and mechanism of MgO dissolution. https://doi.org/10.1016/S0009-2614(99)00909-4.
25. Shih, Y. J., Abarca, R. R. M., de Luna, M. D. G., Huang, Y. H., & Lu, M. C. (2017). Recovery of phosphorus from synthetic wastewaters by struvite crystallization in a fluidized-bed reactor: Effects of pH, phosphate concentration and coexisting ions. Chemosphere, 173, 466–473. https://doi.org/10.1016/j.chemosphere.2017.01.088
26. Martí, N., Pastor, L., Bouzas, A., Ferrer, J., & Seco, A. (2010). Phosphorus recovery by struvite crystallization in WWTPs: influence of the sludge treatment line operation. Water research, 44(7), 2371–2379. https://doi.org/10.1016/j.watres.2009.12.043
27. Uysal, A., Yilmazel, Y. D., & Demirer, G. N. (2010). The determination of fertilizer quality of the formed struvite from effluent of a sewage sludge anaerobic digester. Journal of hazardous materials, 181(1-3), 248–254. https://doi.org/10.1016/j.jhazmat.2010.05.004

28. Pesonen, J., Janssens, F., Hu, T., Lassi, U., & Tuomikoski, S. (2022). Precipitation of struvite using MgSO4 solution prepared from sidestream dolomite or fly ash. Heliyon, 8(12), e12580. https://doi.org/10.1016/j.heliyon.2022.e12580
29. Liu, B., Giannis, A., Zhang, J., Chang, V. W., & Wang, J. Y. (2013). Characterization of induced struvite formation from source-separated urine using seawater and brine as magnesium sources. Chemosphere, 93(11), 2738–2747. https://doi.org/10.1016/j.chemosphere.2013.09.025
30. Crutchik, D., Morales, N., Vázquez-Padín, J. R., & Garrido, J. M. (2017). Enhancement of struvite pellets crystallization in a full-scale plant using an industrial grade magnesium product. Water science and technology : a journal of the International Association on Water Pollution Research, 75(3-4), 609–618. https://doi.org/10.2166/wst.2016.527
31. Pastor, L., Mangin, D., Barat, R., & Seco, A. (2008). A pilot-scale study of struvite precipitation in a stirred tank reactor: conditions influencing the process. Bioresource technology, 99(14), 6285–6291. https://doi.org/10.1016/j.biortech.2007.12.003
32. R. Buchanan, C.R. Mote, R.B. Robinson (2017). Thermodynamics of struvite formation T. https://www.academia.edu/26121340/Struvite_precipitation_thermodynamics_in_source_separated_urine
33. Md.I. Ali, Phil Schneider, Neale Alan Hudson (2003). Nutrient recovery from piggery effluents. https://www.researchgate.net/publication/237626257_Assessing_Nutrient_Recovery_from_Piggery_Effluents
34. Critical Raw Materials - CRM Alliance (2022). http://criticalrawmaterials.org/critical-raw-materials/
35. Aguilar-Pozo, V. B., Chimenos, J. M., Elduayen-Echave, B., Olaciregui-Arizmendi, K., López, A., Gómez, J., Guembe, M., García, I., Ayesa, E., & Astals, S. (2023). Struvite precipitation in wastewater treatment plants anaerobic digestion supernatants using a magnesium oxide by-product. *The Science of the total environment*, *890*, 164084. Advance online publication. https://doi.org/10.1016/j.scitotenv.2023.164084
36. M.S. Romero-Güiza, S. Tait, S. Astals, R. del Valle-Zermeño, M. Martínez, J. Mata-Alvarez, J.M. Chimenos (2015). Reagent use efficiency with removal of nitrogen from pig slurry via struvite: a study on magnesium oxide and related by-products. https://doi.org/10.1016/j.watres.2015.07.043.
37. M. Quintana, M.F. Colmenarejo, J. Barrera, E. Sánchez, G. García, L. Travieso, R. Borja (2008). Removal of phosphorus through struvite precipitation using a by-product of magnesium oxide production (BMP): Effect of the mode of BMP preparation. https://doi.org/10.1016/j.cej.2007.04.002.
38. J.M Chimenos, A.I Fernández, G Villalba, M Segarra, A Urruticoechea, B Artaza, F Espiell (2003). Removal of ammonium and phosphates from wastewater resulting from the process of cochineal extraction using MgO-containing by-product.
39. Ricardo del Valle Zermeño, Jessica Giró Paloma, Joan Formosa Mitjans, Josep Ma. Chimenos Ribera. (2015). Low-grade magnesium oxide by-products for environmental solutions: characterization and geochemical performance. http://hdl.handle.net/2445/143657

40. Awais Bokhari, Suzana Yusup, Saira Asif, Lai Fatt Chuah, Leow Zi Yan Michelle (2020). Chapter 3 - Process intensification for the production of canola-based methyl ester via ultrasonic batch reactor: optimization and kinetic study. https://doi.org/10.1016/B978-0-12-821264-6.00003-6.
41. T.K. Harris, M.M. Keshwani (2009). Chapter 7 Measurement of Enzyme Activity. https://doi.org/10.1016/S0076-6879(09)63007-X.
42. Levenspiel: Chemical Reaction Engineering Third Edition (1999).
43. The Arrhenius Law (2022). https://chem.libretexts.org/Bookshelves/Physical_and_Theoretical_Chemistry_Textbook_Maps/Supplemental_Modules_(Physical_and_Theoretical_Chemistry)/Kinetics/06%3A_Modeling_Reaction_Kinetics/6.02%3A_Temperature_Dependence_of_Reaction_Rates/6.2.03%3A_The_Arrhenius_Law
44. Arthur Frost, Ralph Pearson (1961). Kinetics and Mechanism. https://doi.org/10.1021/j100820a601
45. R. del Valle-Zermeño, J. Formosa, J.A. Aparicio, J.M. Chimenos (2014). Reutilization of low-grade magnesium oxides for flue gas desulfurization during calcination of natural magnesite: A closed-loop process. https://doi.org/10.1016/j.cej.2014.05.089.
46. Nari Park, Hyangyoun Chang, Yeoju Jang, Hyunman Lim, Jinhong Jung, Weonjae Kim (2021). Prediction of adequate pH and Mg2+ dosage using an empirical MgO solubility model for struvite crystallization. https://doi.org/10.1016/j.eti.2020.101347.
47. Giovanni Di Liberto, Farahnaz Maleki, Gianfranco Pacchioni (2022). pH Dependence of MgO, TiO2, and γ-Al2O3 Surface Chemistry from First Principles. https://doi.org/10.1021/acs.jpcc.2c02289
48. Apuntes Cinètica Aplicada I Catàlisi (UB).
49. Chemical Equilibrium (2022). https://chem.libretexts.org/Bookshelves/Introductory_Chemistry/Chemistry_for_Allied_Health_(Soult)/08%3A_Properties_of_Solutions/8.02%3A_Chemical_Equilibrium
50. Crutchik, D., Morales, N., Vázquez-Padín, J. R., & Garrido, J. M. (2017). Enhancement of struvite pellets crystallization in a full-scale plant using an industrial grade magnesium product. Water science and technology : a journal of the International Association on Water Pollution Research, 75(3-4), 609–618. https://doi.org/10.2166/wst.2016.527
51. M. Quintana, E. Sánchez, M.F. Colmenarejo, J. Barrera, G. García, R. Borja (2005). Kinetics of phosphorus removal and struvite formation by the utilization of by-product of magnesium oxide production. https://doi.org/10.1016/j.cej.2005.05.005.
52. M.S. Rahaman, D. S. Mavinic, M.I.H. Bhuiyan & F. A. Koch (2010). Exploring the Determination of Struvite Solubility Product from Analytical Results. https://doi.org/10.1080/09593332708618707
53. M I H Bhuiyan, D S Mavinic, R D Beckie (2010). A solubility and thermodynamic study of struvite. https://doi.org/10.1080/09593332808618857
54. Jose Antonio Mejias, Andrew J Berry, Keith Refson, Donald G Fraser (1999). The kinetics and mechanism of MgO dissolution. https://doi.org/10.1016/S0009-2614(99)00909-4.

55. The rate of a Chemical Reaction (2022). https://chem.libretexts.org/Courses/University_of_British_Columbia/CHEM_100%3A_Foundations_of_Chemistry/15%3A_Chemical_Equilibrium/15.02%3A_The_Rate_of_a_Chemical_Reaction